

KEY ISSUES IN APPLICATION OF COMPOSITES TO TRANSPORT AIRCRAFT

M. Stone
Douglas Aircraft Company

ABSTRACT

Key technical issues in the application of composite materials to transport aircraft are identified and reviewed. The issues involve the major contributing disciplines of design, manufacturing, and processing.

The key issues include: crashworthiness considerations (structural integrity, postcrash fires, and structural fusing), electrical/avionics subsystems integration, lightning, and P-static protection design; manufacturing development, evaluation, selection, and refining of tooling and curing procedures; and major joint design considerations.

The Douglas Aircraft Energy Efficiency (ACEE) composite structures program for which key issues are examined includes the DC-10 rudder, DC-10 vertical stabilizer, and the DC-9 wing study projects.

The Federal Aviation Administration (FAA) interface and the effect on component design of compliance with Federal Aviation Regulation 25 Composite Guidelines are discussed.

INTRODUCTION

The application of composite materials to transport aircraft structures has the potential of providing vehicle systems with significant performance improvements. The performance improvements include weight reduction, increased resistance to fatigue, and improved corrosion-resistance. In addition, reductions in acquisition and life-cycle costs can be realized in selected applications. However, the economic impact of composite components on the user airlines is central to their acceptance. The reliability and maintainability of the composite material systems when subjected to the operating environment of commercial transport aircraft is extremely important to the acceptance of the air carriers. The manufacturer must also be confident of his capability to design and produce composite structures within airplane program scheduling constraints and to meet targeted costs. In addition to acceptance requirements for the manufacturer and airlines, composite structures must conform to special guidelines established by the FAA to ensure compliance with Federal aviation regulations.

The physical, chemical, and mechanical characteristics and properties of advanced composite materials differ significantly from conventional aircraft structure, which affects all aspects of the design. Stress-strain-ductility relationships impose severe constraints on major joint design and structural repair. The material impact resistance will govern the allowable strain levels for damage-tolerant design requirements, and the response of composite materials to environments in which electrical phenomena are present is an important design consideration. Nonmetallic material processing and manufacturing procedures alter facility requirements, and a new component fabrication and assembly cost base must be developed.

A number of key technical problems have emerged during research and development efforts and flight service experience for which solutions must be found to realize the potential of advanced composite materials. To further examine this problem, selected key issues that relate to the development phases of the Douglas-NASA Aircraft Energy Efficiency (ACEE) composite structures program are discussed in detail in the following sections. The discussion includes crashworthiness, electrical/avionics requirements, manufacturing development, and major load transfer considerations.

FEDERAL AVIATION ADMINISTRATION INTERFACE

The certification of structural components for use on civil aircraft requires more extensive testing and associated documentation than for conventional metallic structures. This is in part due to the current minimum data base and lack of maturity of the technology.

An advisory circular for composite materials, released by the FAA, contains guidance information which the FAA considers acceptable for showing compliance with the certification requirements of civil composite aircraft. The advisory circular will be modified periodically to reflect technological advances. The document presently specifies the following with respect to compliance: (1) material and fabrication development, (2) proof of structure static, (3) proof of structure of fatigue/damage tolerance, (4) crashworthiness, (5) flammability, (6) lightning protection, (7) protection of structure, (8) quality control, (9) repair, and (10) fabrication methods. These requirements are indicative of the spectrum of key technology issues to be addressed.

To show compliance with the FAA advisory circular, the following tests and documentation are necessary:

1. **Certification Plan** – This document outlines all the tests and analyses which will demonstrate complete compliance for FAA certification.
2. **Material Allowables Test Program** – This document outlines all the material tests which are necessary to show compliance. It covers such allowables as tension, compression, interlaminar shear, and fatigue, and includes environmental effects such as humidity and temperature.

The material allowables test plan must be approved by the FAA before the test program is begun, and tests must be FAA-witnessed or witnessed by an FAA-designated engineering representative (DER). Test results are submitted to the FAA for approval.

3. **Static and Fatigue/Damage Tolerance Test Program** – Static and fatigue/damage tolerance tests should be conducted on full scale or representative structural components to demonstrate the ultimate strength and the fatigue and damage tolerance capabilities of the structure. All test plans and test results must be approved by the FAA and all tests must be witnessed by the FAA or an FAA DER.
4. **Strength Substantiation** – The advanced composite material structure design must be substantiated by analytical methods to prove structural integrity for ultimate strength, fatigue and damage tolerance capability, crashworthiness, ability to withstand lightning strikes, and any other considerations specified in the advisory circular.



5. **Manufacture and Repair** – All manufacturing and material process specifications for composite materials require FAA approval. Composite material structural repairs which are published in the airplane service repair manuals must also be approved by the FAA.

CRASHWORTHINESS

The objective of FAA criteria for crashworthiness of the airframe is to ensure that occupants have every reasonable chance of escaping serious injury under survivable crash conditions.

Crashworthiness is considered a key issue because airframe structure which utilizes advanced composite materials must provide the same level of safety as conventional construction and because the behavior of composites in a crash situation has not been established. Advanced composites are generally thought of as poor materials for crashworthiness (compared to aluminum) because of their known brittle behavior. However, for many structural configurations, ductility can be shown to not be a crashworthiness factor, and comparable levels of safety can readily be achieved.

The crashworthiness of a structure is measured by its capability to perform three major functions: (1) the reduction of mechanical forces upon impact with the ground or other objects; (2) the capability of the fuselage shell to remain intact to provide the occupants with protection in the event of a postcrash fire; and (3) the maintenance of fuel tank integrity in a crash.

Crashworthiness of aircraft with conventional fuselage shells is enhanced because the aluminum construction possesses the ability to absorb considerable energy through deformation and tearing. This material behavior results principally from the inherent ductility of aluminum. If the aluminum is replaced with an advanced composite material, energy absorption would be reduced and more structural breakup would be expected to occur.

The ductility and energy absorption characteristics of a quasi-isotropic T300/5208 graphite/epoxy composite are compared to those of 2024-T3 in Figure 1 by using typical stress-strain curves for the two materials. Ductility is a direct function of the strain rate, and energy absorption capability is a direct function of the area under the stress-strain curve from zero to the strain rate at failure. Typically, the aluminum could sustain more than 24 times the deformation and has more than 64 times the energy absorption capability of the composite material. However, the total structural response to crash loads is also dependent upon the flexibilities due to the structural arrangements, and the overall performance of full-scale advanced composite structures to crash loads has not been established.

Based on limited tests to date (reference 1), there is encouraging evidence that in a fire, graphite-resin material systems would provide considerably greater burn-through protection for occupants in a nonpunctured composite fuselage shell than present aluminum structure. This protection affords reduced thermal threat, smoke, and toxicity, and extends the time for safe egress.

For wing structures, the goal is to avoid fuel spillage from the integral wing tanks by designing to maintain fuel tank integrity for a reasonable set of crash conditions or off-runway incidents. The following failure conditions must be considered:

1. The tank within the fuselage contour must be protected so that exposure to ground scraping action is unlikely for a wheels-up landing.
2. The tank within the fuselage contour must be capable of sustaining 9-g forward crash loads.
3. Airframe components supported by the main wing box integral tank structure must be designed to break away from the wing box without rupturing the wing tank.

These crashworthiness criteria have been conceptually satisfied for a DC-9 aircraft with an advanced composite wing box structure in a current NASA ACEE study.

The DC-9 center wing box is located inside the fuselage and has a fuel capacity of 3528 liters (932 gallons). The tanks are protected against scraping during a wheels-up landing by the fuselage shell and the heavy main keel member in the wheel well. The lower surface of the wing is 58.4 cm (23 inches) above the lower fuselage loft line at the front spar and 43.2 cm (17 inches) above the lower loft line at the rear spar. In addition, there are two cant panels and a heavy keel member directly under the wing which shield the wing box structure (Figure 2).

In over 15 million flight-hours accumulated by the DC-9 fleet, there has been no damage to the center wing box in survivable incidents because the wing box is protected by the structure under it. Thus, the composite wing box is afforded the same level of protection as the conventional wing box.

Inertia loads of 9 g must be sustained by the wing box structure inside the fuselage. Pressure loads are derived based on a full fuel tank with a 9-g head for this condition. The less ductile characteristics of composites can be accounted for in the detailed design by ensuring positive margins of safety for a 9-g fuel load condition and do not impose any special design problems.

Structural fusing as employed in conventional structures allows specific components to break free at predetermined load values to preclude penetration or other damage to the fuel tank. Pylons, landing gear support fittings, and some flight control fittings fall within this category.

The landing gear may be subjected to loads far in excess of design loads after contact with ditches, runway light standards, or other obstacles involved in off-runway incidents. These incidents are infrequent but must be accounted for in the design to prevent fuel tank rupture in accordance with FAR 25.721. The DC-9 main gear is designed to fail in the gear cylinder for high drag-load conditions, but other fuse points must be utilized for high resultant vertical and drag load combinations. The concept used for the DC-9 composite wing design allows for the main gear to remain intact. The failure will occur aft of the tank boundary in the following sequence:

1. The graphite/epoxy lower cover skin and titanium doubler will fail aft of the rear spar due to overload.
2. The primary restraining load path is then transferred to the two tension bolts attaching the support fitting to the lower bulkhead cap. These two bolts will fail due to overload.
3. The shear bolts attaching the support to the rear spar web will fail in the thin bolt heads as the support fitting breaks free from the rear spar.



4. The upper two bolts and upper cover skin and doubler will bend upward as the intact gear and support fitting rotate upward due to lack of a restraining moment.

A breakaway conceptual design for a composite wing box is illustrated in Figure 3. The composite lower skin and titanium doubler structural margins forward of the rear spar must be maintained at least 10 percent greater than aft of the rear spar. The in-tank aluminum support bulkhead is designed to be 5 percent stronger than the maximum strength of the two lower support fitting attach bolts.

The wing flaps in the landing flap position and wing-mounted engines will contact the runway if the landing gear collapses during landing. FAR 25.963 specifies that fuel tank integrity must be maintained for this condition.

The DC-9 wing flap is attached to the main composite wing box at three support locations. Four bolts attach the hinge fittings at each location (see Figure 4). The lower two bolts at each hinge fitting are necked down outside the tank boundary to form a fuse point for high tension loads caused when the flap structure strikes the runway. The fitting will then rotate about the two upper bolts and the wing tank will not rupture. The primary design task is to ensure that the flap bulkhead inside the tank is stronger than the fuse point of the attach bolt.

ELECTRICAL AND AVIONICS REQUIREMENTS

The use of graphite/epoxy composite structures on aircraft instead of conventional aluminum structures has necessitated the development of new design practices for electrical and avionics subsystems, especially for lightning protection designs. Electrical currents and heat are easily conducted by conventional skin panels made of aluminum. Aluminum panels are frequently used to conduct electrical elements of ground return paths and antenna elements. The metal skin also provides good electromagnetic shielding for critical electronic components and good conductive paths for lightning currents. Recent research and development programs sponsored by Government and industry have defined some of the conductive characteristics of graphite composite structures (references 2 and 3). They are far less conductive than aluminum structures, and investigations were made to determine if composite structures are satisfactory for shielding and lightning protection. Also, the low cost and lightweight aspects of the graphite composite structure design must be especially considered in integrating electrical and avionics subsystems and in incorporating lightning protection hardware.

Early test results (reference 4) indicated that certain types of graphite composite structures could be severely damaged by lightning strike attachment (Figure 5). Graphite composite structures are conductive enough to attract lightning strike current in a similar manner as aluminum structures, and yet they are not conductive enough to transfer the high energy involved in a severe lightning strike. The flow of lightning currents across structural joints also becomes a major design consideration. A composite structure joint damaged by lightning test is shown in Figure 6. Two new low cost and lightweight lightning protection design concepts have been developed (reference 5) and successfully demonstrated in several composite structure programs. They are the isolation concept and the conductive concept.

Isolation Design Concept

The isolation design concept is based on isolating the graphite composite structure from lightning current flow paths by covering the surface of graphite or boron composite skins with high dielectric strength material to prevent the swept-stroke/restrike lightning channel from attaching to the skins. The dielectric material may be in the form of a film or coating and its thickness will depend upon the dielectric strength required. The design principle is illustrated in Figure 7.

During the swept-stroke event, the lightning channel is forced to remain attached to a forward metal surface as it bends over the composite skin panel by the forward movement of aircraft. The lightning channel has an IZ impedance voltage drop V_c . There is also a breakdown voltage V_b between the lightning channel and the composite skin panel. As the channel is swept rearward, the portion of lightning channel lying over the composite panel is lengthened and V_c is increased. When V_c exceeds V_b , a new lightning attachment can occur. Therefore, by incorporating a dielectric layer over a composite skin panel, a certain span of the composite skin panel can be protected from the swept-stroke/restrike attachment.

The isolation concept for lightning protection is utilized on the DC-10 composite rudder design. Douglas is currently under contract with NASA to build several graphite composite DC-10 upper-aft rudders for flight service evaluation. The rudder component is located in the upper-aft extremity of the aircraft and requires both direct and swept-stroke/restrike lightning protection. The overall rudder lightning protection design is illustrated in Figure 8. Four P-static discharger installations are located at its trailing edge area and are electrically connected to aircraft metal structure. The rudder component does not enclose electrical/avionics components and therefore does not require electromagnetic shielding protection.

The isolation design concept proved to be the most suitable for the lightning protection of this composite structural component. Two aluminum straps were installed around the fiberglass tip and trailing edge to divert and guide direct lightning strike currents to the forward rudder metal structures through a bonding jumper installation. The four P-static discharger installations were electrically connected to these aluminum straps. A dielectric coating system was applied over the graphite skin panel surface for the swept-stroke/restrike protection. The graphite composite structures are thus completely isolated from lightning stroke currents. Laboratory-simulated lightning tests have demonstrated the successful operation of this isolation design.

Conductive Design Concept

The most practical and efficient lightning protection design for large composite structure applications is to utilize the conductive characteristics of the baseline composite structures such as skin panels and joints in the overall aircraft lightning protection design.

A metal strip protection system as illustrated in Figure 9 can be used to provide direct lightning stroke protection to graphite composite structures located in the direct lightning strike region. The graphite composite skin panel surrounding these metal strips will conduct a certain amount of lightning current since it serves as a parallel path from an electrical viewpoint. However, a careful design of the fastener installation and the composite skin panel installation can limit the amount of lightning current flowing in the composite skin panel to an acceptable level.

Proper use of the conductive properties of graphite composite structures for transferring lightning currents will eliminate the requirement for additional lightning protection material to conduct lightning currents through the lightning current transfer region. This conductive design concept is being considered for application in the DC-9 composite wing box program and other advanced program proposals.

An "all-composite" aircraft will retain many metal substructures which can be used to conduct lightning currents. An important design consideration is the proper introduction of lightning currents through metal-to-composite and composite-to-composite structural joints, so that the structural integrity of these points will not be affected by the flow of lightning currents. A proposed lightning protection concept for the DC-10 composite vertical stabilizer is illustrated in Figure 10.

MANUFACTURING DEVELOPMENT

The selection of the manufacturing method for composite fabrication is an integral part of the design process and as such is the most significant element in the cost of composite structures.

Autoclave and vacuum bag curing (reference 6), matched die pressing (reference 6), and thermal expansion cure techniques (reference 7) have all been used successfully for a variety of structural elements. Part size, geometry, complexity, and required quantity are all considerations in the selection of a fabrication process.

In the preliminary design phase of the DC-10 graphite rudder, a rib-stiffened design was selected (Figure 11) as the most advantageous concept due to minimum weight and adaptability to a thermal expansion trapped rubber curing process which permitted the molding and cocuring of the rudder structural box in one piece (skins, spars, and ribs).

A standard oven was satisfactory for curing, and repeatability of the process was possible with minimal tool refurbishment. However, there were disadvantages of the process which are covered below.

Four significant problems were encountered during fabrication of several development subcomponents (Table 1). During the first cure cycle, excessive pressures were developed in the Silastic J rubber mandrels, estimated at 6.89 to 10.3 MPa (1000 to 1500 psi), and two of the 2.54-cm- (1-inch-) diameter tooling bolts retaining the side plates failed in tension and bending. The heat-up rate was also very slow due to the mass of the mold tool. The subcomponent tool and mandrels are shown in Figure 12 (tool side plates have been removed for clarity).

The internal metal mandrels were redesigned and the rubber mandrels were recast using Dapocast 38-3 rubber for the second cure cycle. The redesigned metal mandrels allowed for the correct volume of rubber and utilized internal electrical heaters to increase the heat-up rate and thus reduce the thermal gradients through the assembled tool and laminate during the cure cycle. In addition, the redesigned mandrels were a multipiece aluminum alloy rather than the one-piece steel mandrel. The aluminum alloy promoted faster internal heat transfer and the multipiece construction facilitated mandrel removal.

To verify the revised tooling, a fiberglass subcomponent was successfully cured during the second cure cycle (Figure 13). However, considerable shrinkage of the rubber mandrels was discovered after they were removed from the three rib-bays. The mandrels shrank approximately 0.635 cm (0.25 inch) on the chordal dimension of 60.96 cm (2 feet).

The cure of a third part was attempted using the rubber mandrels which shrank during the second cycle. The cured laminates had poor fiber collimation and regions of large resin accumulation because the undersized mandrels failed to expand to the required pressure threshold until the material was well into its gel period during the cure cycle. The shrinkage problem was resolved by inserting a coarse wire-mesh screening in the pieces of cast rubber. The screening provided a mechanical restraint against shrinkage and the rubber mandrels were dimensionally stable thereafter. The wire-mesh screening, as utilized on the full-scale tool mandrels, is shown in Figure 14.

During fabrication of the first three subcomponents, rubber mandrel segments were particularly difficult to remove. Although the mandrels were liberally sprayed with a release agent prior to assembly, the temperatures and pressures sustained during the cure cycles effectively bonded the rubber segments to each other, to the metal mandrels, and to the laminate. This problem was resolved by coating the segments with a 0.08-mm (3-mil) Teflon tape at all appropriate faying surfaces.

After the metal mandrels were modified to incorporate internal heaters and the rubber mandrels were stabilized with metal screening and coated with Teflon, four additional subcomponents were fabricated for final tool and processing verification. Since no problems were encountered, construction of full-scale rudder tooling was initiated. Essential details of the full-scale rudder molding die are shown in Figure 15.

Four graphite rudder boxes were cured during the full-scale proof-of-tooling phase. Additional problems encountered during cure of the first three full-scale boxes are summarized in Table 2. After the second unit had been cured, it was concluded that the rubber mandrels had been cast slightly oversize. Although the tooling bolts were carefully torqued, the curing tool could not be fully closed. Gaps near the rear-spar flanges resulted in laminates that had high void content in that locality and poor dimensional control. These problems were remedied by recasting the rubber mandrels to the correct size.

The subsequent cure cycle was completed and resulted in a part with good laminate resin and void contents and part dimensions within engineering tolerance requirements. The fabrication of 10 graphite rudder boxes was then completed for flight service. A lineup of rudders during the final assembly process is shown in Figure 16.

A rudder modification program was conducted to develop and demonstrate manufacturing processes in order to provide a cost-competitive position between the graphite rudder and the metal unit it replaces.

Changes made to reduce the unit rudder cost included revisions in the rudder unit itself and in the fabrication and assembly tooling.

The rudder material for spars, ribs, and skin doublers was changed to a bidirectional weave fabric from 7.62 cm (3 inch) unidirectional tape. The basic skin panels will be fabricated from a unidirectional

weave fabric in lieu of the original tape material. Fabrication of rudder box details will be expedited by the use of a die trimmer tool and clicker press for preparing rudder box element flat patterns with the subsequent predensification operation accomplished simultaneously in gang fashion on a vacuum table.

Additional manufacturing revisions included the modification of the temperature monitoring and control system (Figure 17) into a computer-controlled automated cure process system and an additional assembly jig to perform some operations apart from the final assembly jig.

Cost estimates based on the above improvements resulted in the following data projections:

1. The combined unit cost (recurring only) of manufacturing the graphite/epoxy mold assemblies for the last three rudder units (i.e., 18th, 19th, and 20th) is 1110 man-hours.
2. The breakeven point of graphite/epoxy production rudders with conventional production rudders based on an economic analysis of recurring costs only is projected to occur between 50 and 70 units.

The comparison of total recurring labor hours for the first set of 10 rudders for units 11 through 20 is shown in Figure 18.

MAJOR JOINT DESIGN

In realizing the full potential of composite materials in lightweight aircraft structures, it is particularly important to ensure that the joints, either bonded or bolted, do not reduce the efficiency of the structure. The joining problem is far more severe with composites than with conventional metals such as aluminum, titanium, and steel because the high-specific-strength fibers and filaments are relatively brittle. They have little capacity to redistribute loads and none of the ductility of a yielding metal to mask a multitude of design approximations. Specifically, the graphite and boron/epoxy composites fail at a strain no greater than 1 percent whereas aluminum alloys, which yield at a strain of about 0.7 percent, typically stretch without failing more than 10 percent. While the component fibers and filaments behave linearly elastically to failure, there is a significant nonlinear behavior associated with delaminating the resin matrix in the actual composite. These delaminations can often soften stress concentrations to about half the concentrations of an equivalent homogeneous orthotropic material (reference 8), and this benefit should be accounted for in design. However, this relief falls far short of the complete ductility around stress concentrations in the metal alloys prior to failure.

This ductility of metals has come to be relied upon in design practice. An example of this is to be found in the multiple-row bolted joints used to splice wing skins at the centerline or sides of the fuselage. At ultimate load, the metal yields sufficiently for each bolt to carry its proportional share of the load. If this were done in composites, however, most of the load transfer would be confined to the outer rows of bolts, leaving the inner rows very lightly loaded, even at failure (Figure 19). This represents a severe design problem for highly loaded structures and is a key situation requiring examination and solution early in the design process. This load-sharing problem is so acute for composites that testing (reference 8) has shown that two rows of bolts can transfer no more than

about 10 percent more load than a well-proportioned single-row bolted joint. Therefore, it is unlikely that one will see many applications of more-than-two-row bolted joints in composites. This is quite a departure from standard metal practice.

Adhesive bonded joints also undergo nonuniform load transfer which comes from three basic sources. The first is adherend flexibility, which is explained in Figure 20 in terms of the adherend differential movement across the adhesive layer. The adhesive therefore develops a lightly loaded elastic trough between the effective load transfer zones at the ends of the overlap. While it may seem at first sight that the joint would be improved by redesign to raise the adhesive stress in that area, it should be considered that such an increase in joint strength is found by test (reference 9) to be associated with a reduction in service life and environmental resistance because of cumulative creep damage. A minimum expanse of elastic trough is needed to keep the stress in the middle so low that the adhesive there will never creep, so that the joint strength will not degrade in service. One should, however, then try to work each end of the joint adhesive equally to maximize the load transfer. This cannot be done if there is an adherend stiffness imbalance, as described in Figure 21. The adhesive shear strains are intensified at the ends from which the softer (less stiff) adherend extends. The same end of the joint is critical whether the joint load is tensile or compressive. This stiffness imbalance has been considered in the design of the major fittings for the DC-10 composite vertical stabilizer, in which the titanium fitting thickness at the end of the bonded overlap has been set to match the extensional stiffness of the composite at the other end. A further source of adhesive inefficiency is adherend thermal mismatch (Figure 22), which is acute for the aluminum-to-graphite/epoxy combination joints and still significant for titanium-to-boron/epoxy joints. This problem arises because high-strength adhesives are customarily cured at temperatures far above their operating temperature.

The important characteristic of the so-called thermal stress imbalance is that the critical end of the joint changes with the direction in which the load is applied. With all other variables held constant, this problem becomes progressively more severe with increasingly thick adherends to the extent that some joints are observed to break apart while cooling down in the autoclave after the adhesive is cured without the application of any external load. The only solution to this problem is to use a scarf joint with very small scarf angle, as is proposed for the major fittings on the DC-10 graphite/epoxy vertical stabilizer described later in this section.

The exact thicknesses at which each of these potential problems becomes intolerable are subject to so many variables that analysis is needed to differentiate between "thin" adherends, for which the bond is much stronger than the adherends, and "thick" adherends for which the bond is weaker. A number of suitable analyses for this task have been developed under contract to NASA Langley (references 10 to 14) using an elastic-plastic adhesive model. These are now used widely throughout the aerospace industry. These analyses rely on closed-form solutions and the associated Fortran IV digital computer programs are quick to run, requiring little input.

The remaining dominant characteristic of adhesive-bonded joints is the peel stresses developed in association with the shear stresses. Like the shear stresses, the peel stresses are maximized at the ends of the joint. The inner laminate split apart locally due to the peel stresses, thereby destroying the shear transfer capacity between the inner and outer plies. This overloads the outer filaments, which fail in tension. This problem can be alleviated by tapering the outer adherends to reduce peel stress. Thickness discontinuities should not exceed about four plies of composite.

The relative use of a variety of basic bonded joint types is summarized in Figure 23. As the load level and adherend thickness increase, progressively more complex joints are needed. On the other hand, one should never use a more complex joint type than is necessary. The scales shown vary with both material and environment but, as a general rule, stepped-lap joints become necessary at an adherend thickness of about 0.5 cm (0.20 in.), while tapered-lap joints are suitable up to 0.3 cm (0.12 in.), and double-lap or double-strap joints suffice for about 0.2 cm (0.08 in.).

A bonded joint is utilized to transfer the load between the fuselage support structure and the stabilizer box spars on the DC-10 vertical stabilizer-fuselage interface joint. The DC-10 aluminum vertical stabilizer box, shown in Figure 24, is a multispar, multirib structure in which the spar caps resist bending loads and skin panels resist both torque shear loads and local air loads. The extruded spar caps have integrally machined attach fittings at the root ends through which eight bolts attach the upper stabilizer to its support structure.

In the metal design (Figure 24), bending loads are concentrated into four pairs of extruded aluminum spar caps. These caps have integrally machined attach fittings at their root ends, through which eight bolts transfer the cap loads to the lower structure.

For interchangeability reasons, the design for the composite vertical stabilizer is constrained to attach at the existing eight bolt locations, with the same basic four spar structural configuration being retained.

Of the many configurations investigated, seven major variations are shown in Figure 25. Weight estimates for five of these are given in Table 3. From this study it was evident that the all-composite wrap-around concept promised to be the lightest and most efficient design. This configuration, together with the titanium scarf joint concept, has been carried into the test program to determine the joint concept which will form the basis for the final design.

All-composite design represents the minimum-weight solution, but also poses a considerable technical challenge. Basically, the highly unidirectional spar cap material is divided to form a loop at its end through which the tension bolt passes. The layers are not continuous around this loop, but overlap to form an end plate which is twice as thick as the adjacent cap material. In the test component, this end plate has a thickness of 4.7 cm (1.85 inches) which is greater than any previously incorporated in an aircraft component. A satisfactory cure cycle for thicknesses up to 5.08 cm (2 inches) has already been demonstrated at the laboratory level. The bulk of the layup for each fitting is achieved as a separate densified element which is subsequently cocured into the total structural assembly.

The second concept, which incorporates a titanium attach fitting cocured and spliced into the composite assembly, is regarded as a backup solution in the event that the all-composite approach is not found acceptable (Figure 26). Titanium is used in preference to aluminum because its lower thermal expansion is more compatible with the graphite/epoxy material. This allows the two materials to be spliced in a cocured operation, without inducing unacceptably high residual thermal stresses in the adherends or at the adhesive interface. The bathtub end is similar to the existing aluminum design and does not present a design problem.

The titanium fitting transfers the load into the composite structure by means of a double-sided scarf joint, both titanium and graphite being tapered in the joint region. The titanium is inserted within the

laminate layers during the primary cure cycle, with FM300 adhesive film between the material faying surfaces.

Characteristically, the scarf joint does not have the nonuniformity of adhesive shear stress, which is a feature of lap-type joints. However, perfectly uniform stress is not possible where stiffness imbalance and thermal mismatch exist between the two ends of the joint. Stiffness imbalance is avoided by matching the extensional stiffness (EA) of the titanium and composite materials throughout the length of the joint; however, the thermal expansion difference between the two materials must be accounted for. Assuming that the adhesive is initially cured at 177°C (350°F), there is a temperature differential of 138°C (280°F) at room temperature, 21°C (70°F), increasing to 213°C (415°F) each time the aircraft climbs to altitude. This represents a severe fatigue condition, occurring on every flight.

An analysis was conducted which utilized the elastic-plastic behavior of the adhesive and employed the adhesive stress-strain curve in an idealized form amenable to mathematical treatment. A sample printout from this program is given in Figure 27.

The analysis was conducted to cover a range of service temperatures from -57°C (-70°F) to 82°C (180°F) by treating the T-shaped joint as a flat element. The resulting joint configuration was designed for high margins of safety to allow for the possibility that regions of disbond might occur in the adhesive joint during the life of the component. The analysis was conservative because at temperatures approaching the cure temperature there is considerable alleviation due to the rapid creep and low modulus of the adhesive. These factors, taken in conjunction with the fail-safe design condition that the loss of any one complete spar shall be considered, ensures that the joint design will not allow catastrophic failure of the structure.

CONCLUDING REMARKS

As composite technology has matured, various problems have arisen which are unique to the material system. Many of the problems became key issues relevant to the successful application of composites to transport aircraft. Some key issues relating to the NASA ACEE composite structure program have been summarized in this paper.

The successful application of composite materials to primary structure will depend to a large extent on the ability of the material to meet or exceed the crashworthiness capability of conventional aluminum structures. This has not been demonstrated for the overall performance of full-scale-composite structures at this time but some experimental evidence to date indicates better burn-through protection for postcrash fires.

Research into composite electrical/avionics requirements has provided a data base for the successful lightning protection design of a variety of structural components. Due to the poor electrical and thermal conductivity characteristics of composite materials and the different requirements (position geometry, interfacing subsystems, etc.) which must be satisfied, generalized solutions are not available at this time. However, structural hardware has been designed and demonstrated to provide the necessary degree of successful lightning protection.



Design and manufacturing engineers have a broad selection of fabrication methods and processes available to them for composite hardware manufacture. It is the close interface between component design and fabrication that is essential for low-cost hardware fabrication. The manufacturing issue is not one of producing a workable component but of producing cost-competitive hardware that satisfies all design criteria and requirements.

Joints in aircraft structure are expensive both in weight and construction cost. Composite materials afford the designer an opportunity to minimize the number of joints in a structure but the brittleness and low interlaminar tension characteristics of the composite material impose constraints that require care and finesse in successful joint design.

REFERENCES

1. Hognat, Jacques: Flammability and Fire Resistance of Metallic and Non-Metallic Materials. National Symposium on Fire Safety Aspects of Polymeric Materials, June 1977.
2. Kung, J. T.; and Amason, M. P.: Lightning Conductive Characteristics of Graphite Composite Structures. Douglas Paper 6583, Presented to the 1977 IEEE International Symposium on Electromagnetic Compability, August 1977.
3. Composite Forward Fuselage Systems Integration Program, Second Quarterly Progress Report. AFFDL Contract F33615-76-C-5439, General Dynamics, October 1977.
4. Goodrum, G. T.: Lightning Protection for Advanced Composite Aircraft Structures. SAE Paper 700935, Presented at 1970 Lightning and Static Electricity Conference, December 1970.
5. Kung, J. T.; and Amason, M. P.: Lightning Protection Concepts for Advanced Composite Structures. Douglas Paper 6477, Presented to the 1976 IEEE International Symposium on Electromagnetic Compatibility, July 1976.
6. Plastics Engineering Handbook, Third Edition. The Society of Plastics Industry, Inc., Reinhold Publishing Co. New York, N.Y.
7. Purvis, N. B.: Advanced Composite Rudder Development and Fabrication for the DC-10. Douglas Paper 6427, Presented to American Ceramic Society, October, 1975.
8. Hart-Smith, L. J.: Bolted Joints in Graphite-Epoxy Composites. NASA CR-144899, June 1976.
9. Thrall, E. W., Jr., et al.: Primary Adhesively Bonded Structure Technology (PABST), Phase 1b: Preliminary Design. Technical Report AFFDL-TR-76-141, December 1976, pp. 149-151.
10. Hart-Smith, L. J.: Analysis and Design of Advanced Composite Bonded Joints, NASA CR-2218, January 1973.
11. Hart-Smith, L. J.: Adhesive-Bonded Double-Lap Joints. NASA CR-112235, January 1973.
12. Hart-Smith, L. J.: Adhesive-Bonded Single-Lap Joints. NASA CR-112236, January 1973.
13. Hart-Smith, L. J.: Adhesive-Bonded Scarf and Stepped-Lap Joints. NASA CR-11237, January 1973.
14. Hart-Smith, L. J.: Non-Classical Adhesive-Bonded Joints in Practical Aerospace Construction. NASA CR-112238, January 1973.

TABLE 1.- SUBCOMPONENT DEVELOPMENT PROBLEMS AND SOLUTIONS

CURE CYCLE	PROBLEMS	CAUSE	SOLUTION
1	2.5-cm (1-IN.) DIAMETER TOOLING BOLTS FAILED.	EXCESSIVE PRESSURE.	CHANGED RUBBER FORMULATION. REDUCED RUBBER VOLUME.
2	RUBBER MANDRELS SHRUNK.	CREEP BEHAVIOR UNDER CURING HEAT AND PRESSURE.	REMADE RUBBER MANDRELS WITH METAL INCLUSIONS TO STABILIZE DIMENSIONS.
3	POOR FIBER COLLIMATION AND LARGE ACCUMULATIONS OF RESIN.	LAMINATE CURED WITH INADEQUATE PRESSURE.	ADDED ELECTRICAL HEATERS WITHIN METAL MANDRELS FOR INSIDE-OUT HEATING.
4	RUBBER MANDRELS STUCK.	CURING HEAT AND PRESSURES.	ADDED TEFLON TAPE AT FAYING SURFACES.
5-8	NONE	-	-

TABLE 2.- FULL-SCALE RUDDER DEVELOPMENT PROBLEMS AND SOLUTIONS

CURE CYCLE	PROBLEM	CAUSE	SOLUTION
1-2	VOIDED REGIONS NEAR REAR SPAR. POOR LATERAL DIMENSIONAL CONTROL.	UNABLE TO CLOSE MOLD BECAUSE OF OVERSIZED RUBBER MANDRELS.	RECAST RUBBER MANDRELS.
3	REGIONS OF SKIN CURED WITH INADEQUATE PRESSURE.	EXCESSIVE DENSIFICATION STAGING OF SKINS. DEVELOPED PRESSURE TOO LATE IN CURE CYCLE.	REDUCED DENSIFICATION CONDITIONS. EXPANDED RUBBER SOONER WITH INTERNAL HEAT.
1-3	LOCALIZED CRACKS IN FRONT SPAR.	INDUCED STRESSES DURING COOL-DOWN.	ADDED LOCAL LAYERS. IMPROVED PREFORM TECHNIQUE TO REMOVE ECCENTRICITIES.
4	NONE	-	-

TABLE 3.- REAR SPAR CAP WEIGHT COMPARISONS

ATTACH FITTING CONCEPT	METAL END FITTING ⁽¹⁾ LENGTH cm (IN.)	WEIGHT, kg (LB)		
		INBOARD 81.3 cm (32 IN.)	OUTBOARD 609.6 cm (240 IN.)	TOTAL 690.9 cm (272 IN.)
BASELINE (ALL ALUMINUM)	N/A	9.95 (19.5)	9.62 (21.2)	18.5 (40.7)
ALL COMPOSITE WRAP-AROUND SECTION	N/A	4.85 (10.7)	6.67 ⁽²⁾ (14.7)	11.5 (25.4)
ALUMINUM END BUTT-SPLICE	44.2 (17.4)	11.88 (26.2)	6.67 ⁽²⁾ (14.7)	18.6 (40.9)
ALUMINUM END LAP-SPLICE	52.1 (20.5)	11.39 (25.1)	6.67 ⁽²⁾ (14.7)	18.1 (39.8)
TITANIUM TRANSITION SPLICE MEMBER	37.1 (14.6)	7.48 (16.5)	6.67 ⁽²⁾ (14.7)	14.2 (31.2)
TITANIUM END WITH BONDED SPLICE	49.5 (19.5)	6.99 (15.4)	6.67 ⁽²⁾ (14.7)	13.7 (30.1)

(1) MEASURED FROM STATION $Z_{FR} = 292.255$ TO OUTBOARD END FITTING.

(2) BASED ON AMC 7185 REAR SPAR CAP "EA"

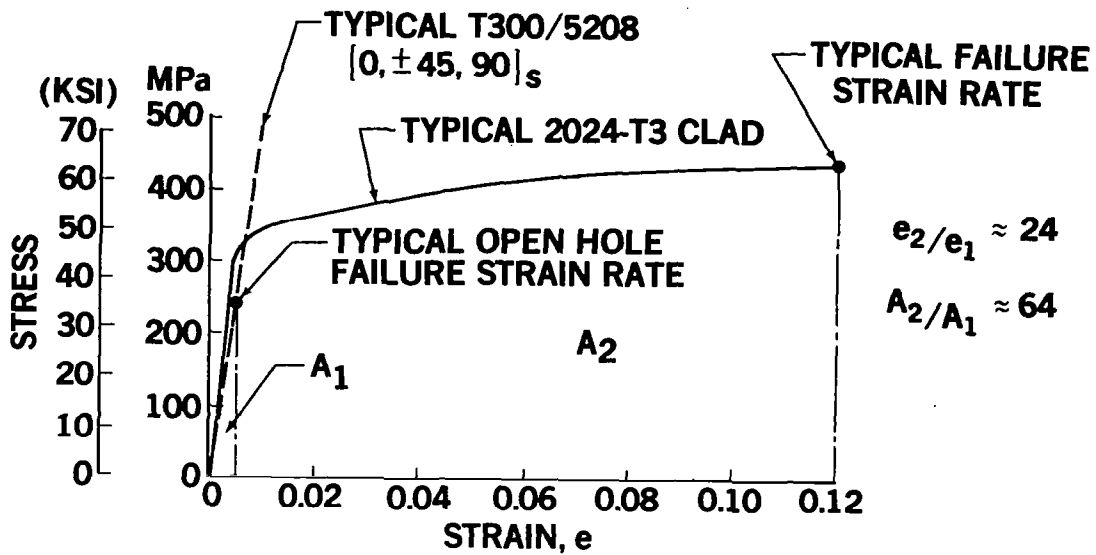


Figure 1.- Stress-strain relationship of graphite/epoxy and aluminum materials.

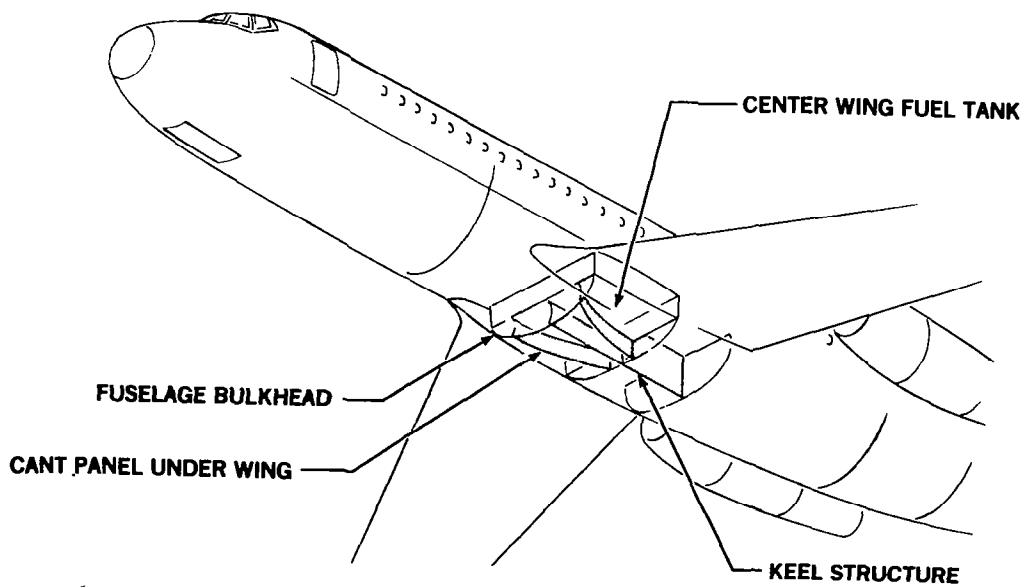


Figure 2.- Protection of center wing fuel tank structure.

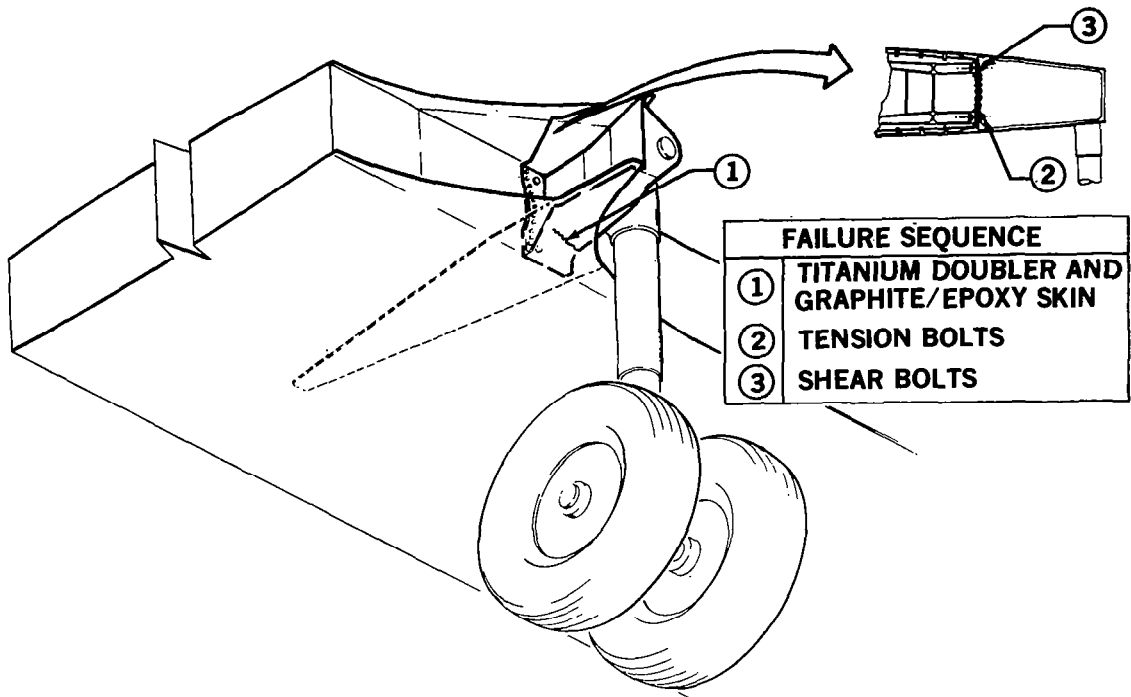


Figure 3.- Main gear breakaway features for structural overload.

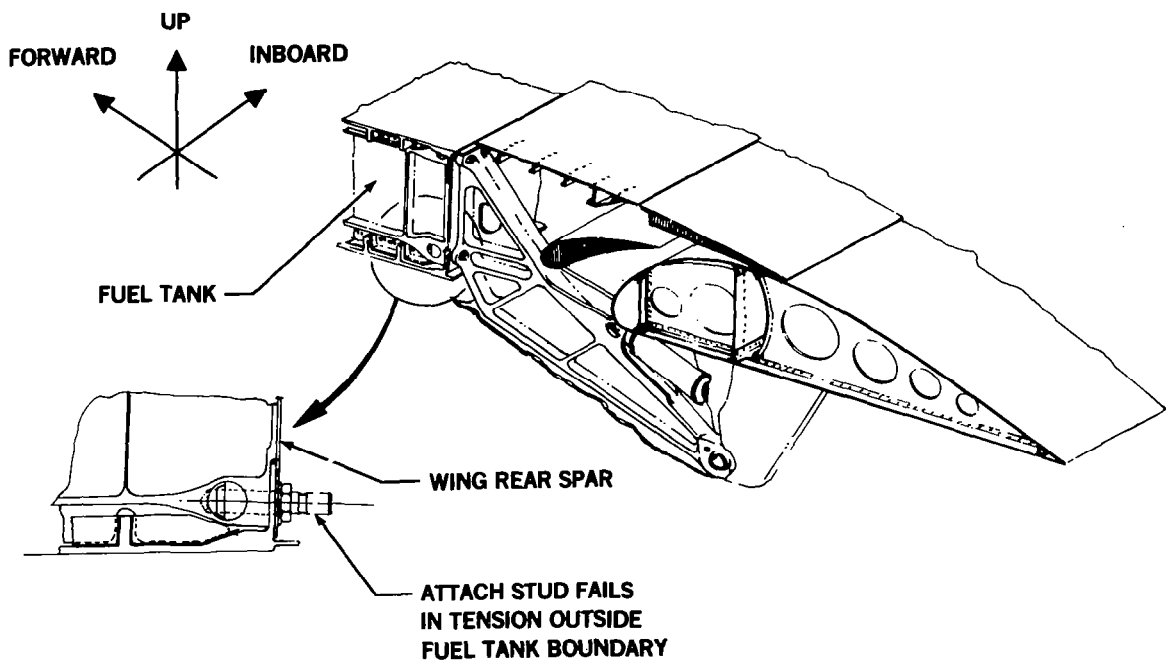


Figure 4.- Flap support structure overload breakaway design.

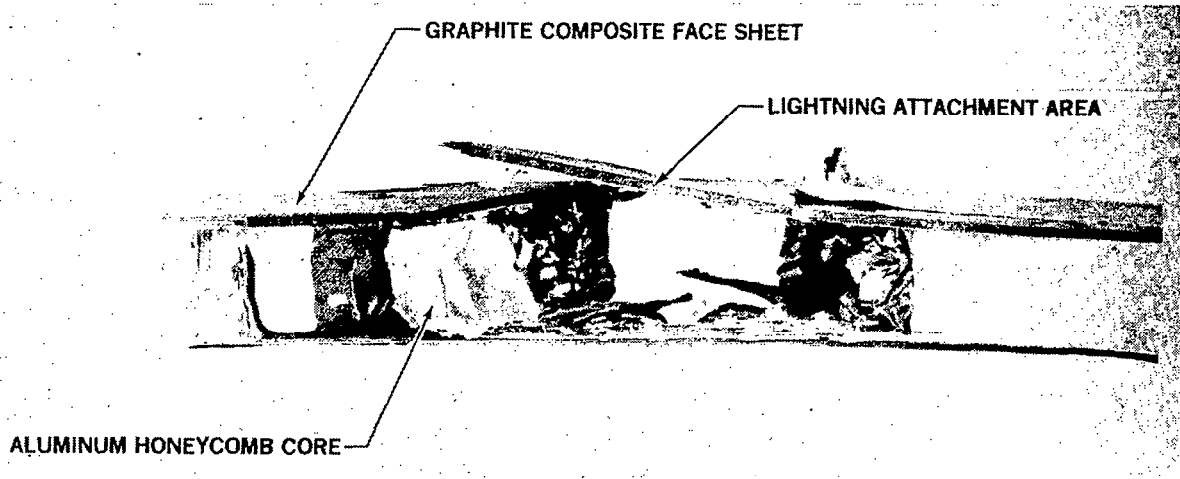


Figure 5.- Lightning strike attachment damage to a sandwich graphite composite panel with aluminum honeycomb core.

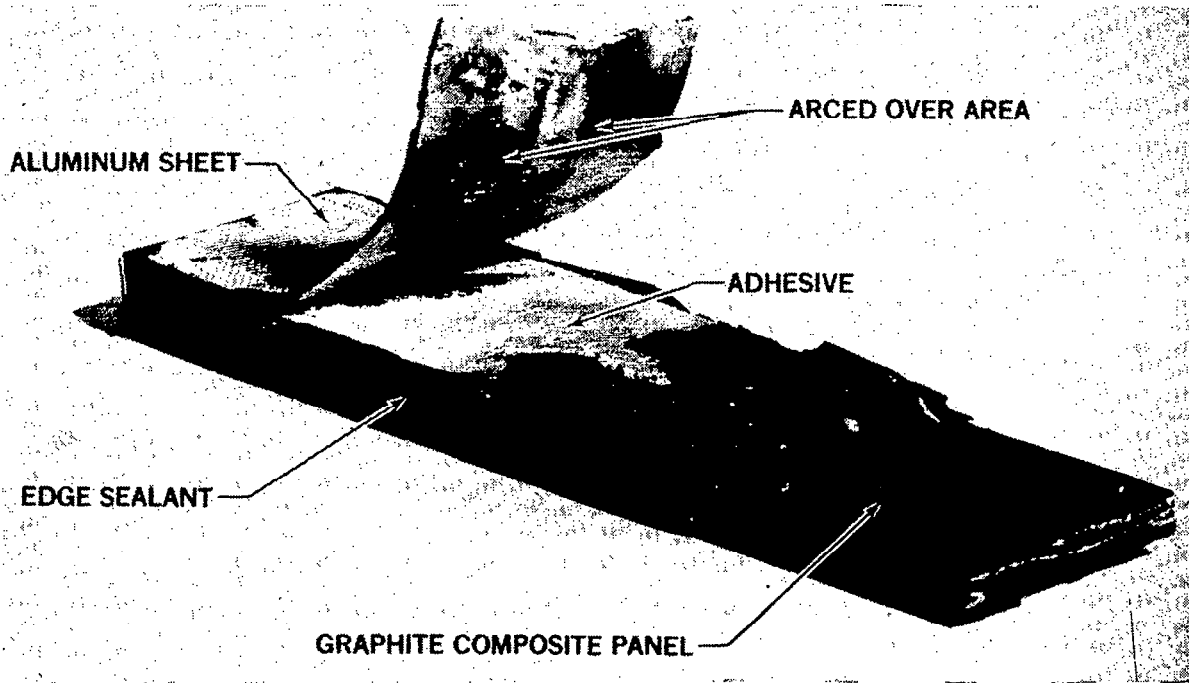


Figure 6.- Metal-to-composite joint damaged after lightning test.

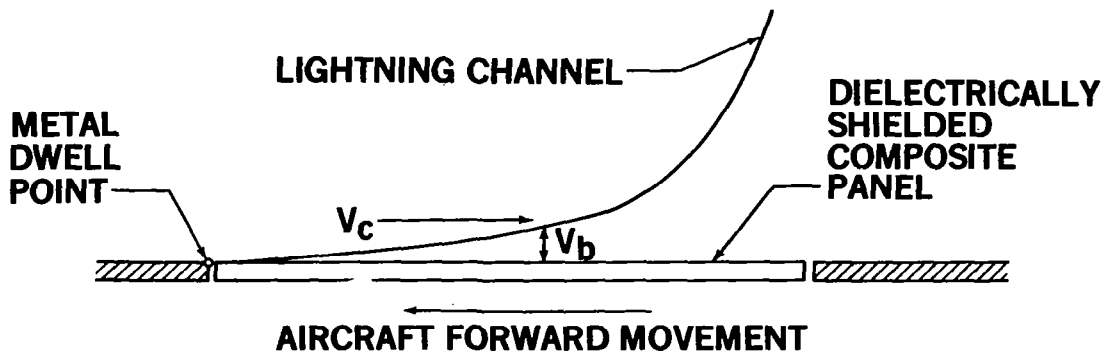


Figure 7.- Swept-stroke attachment criteria.

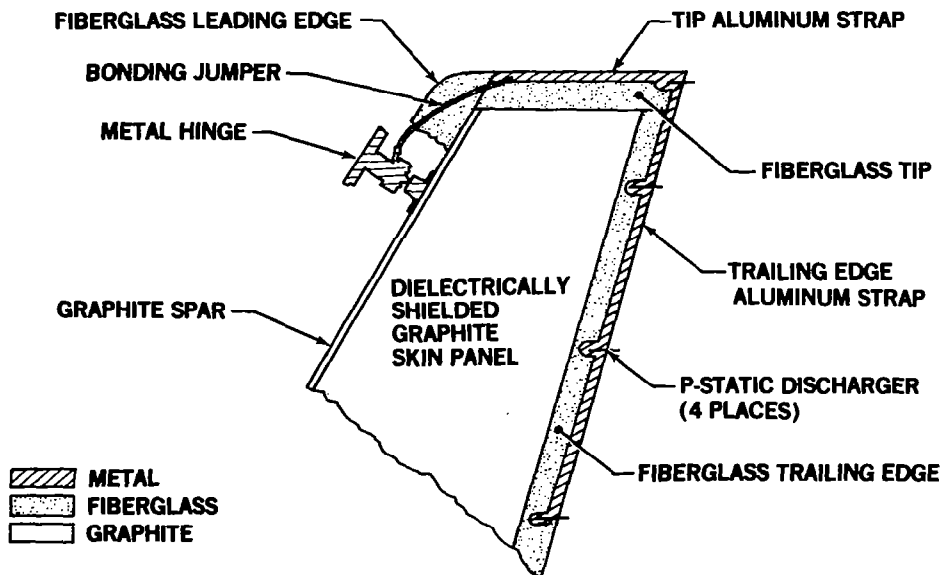


Figure 8.- DC-10 composite rudder lightning protection.

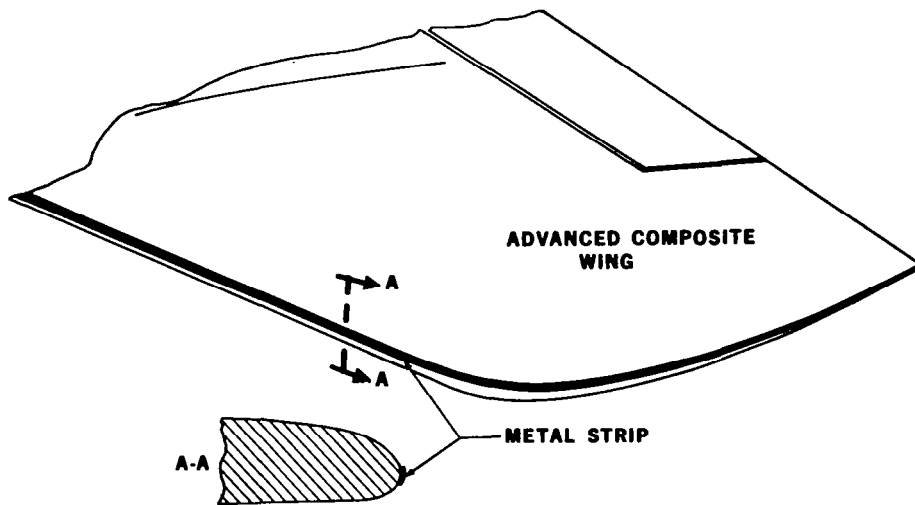


Figure 9.- Lightning strip protection system.

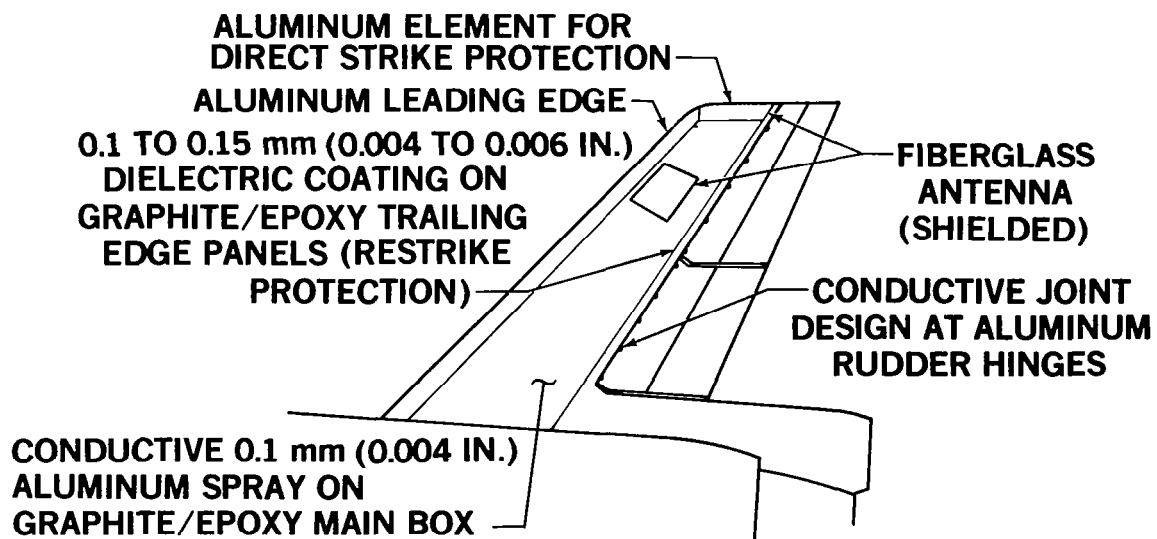


Figure 10.- DC-10 composite vertical stabilizer.

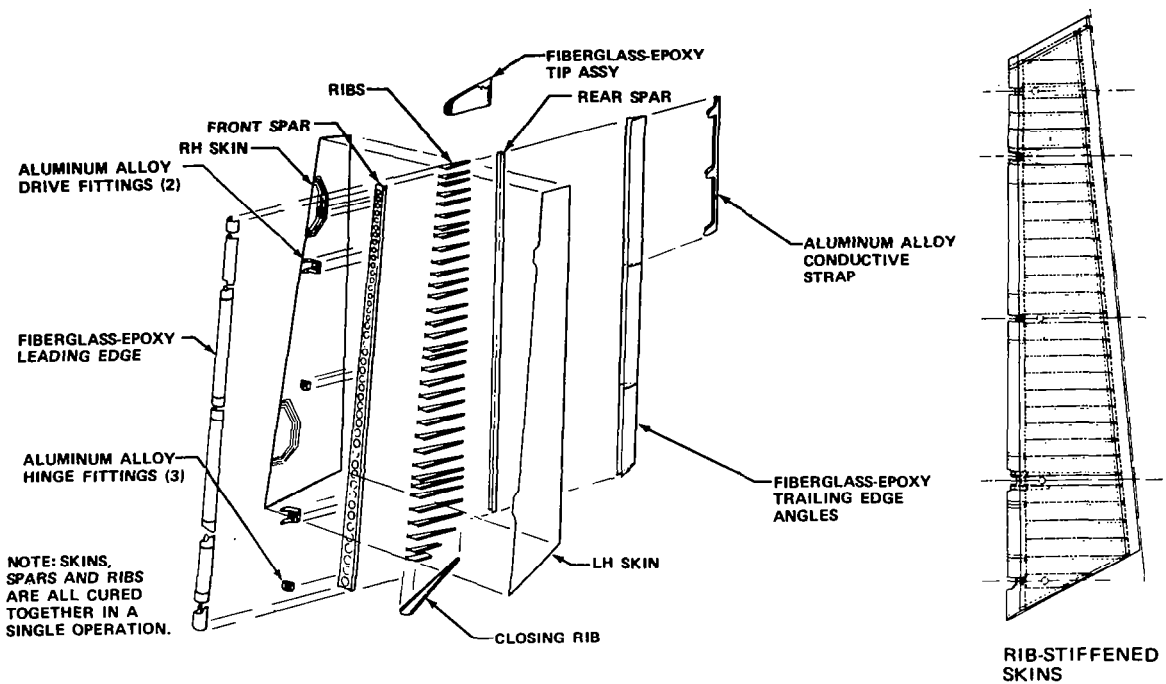
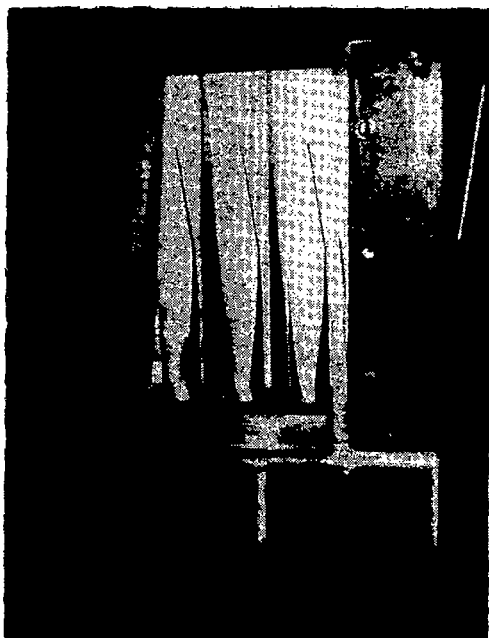


Figure 11.- Rib-stiffened graphite/epoxy rudder.



<u>PROBLEMS</u>	<u>SOLUTION</u>
EXCESSIVE PRESSURE	REDUCED RUBBER VOLUME
RUBBER MANDRELS SHRUNK	REMADE RUBBER MANDRELS WITH METAL INCLUSIONS TO STABILIZE DIMENSIONS
POOR FIBER COLLIMATION AND LARGE ACCUMULATIONS OF RESIN	ADDED ELECTRICAL HEATERS WITHIN METAL MANDRELS
RUBBER MANDRELS STUCK	ADDED TEFLON TAPE AT FAYING SURFACES

Figure 12.- Trapped rubber process development.



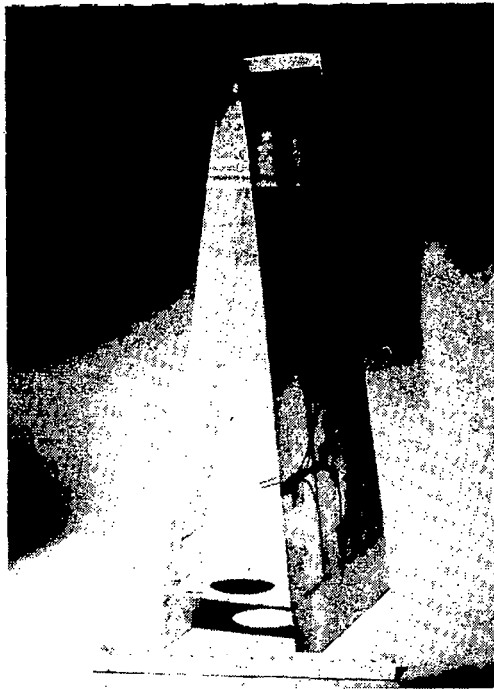


Figure 13.- Fiberglass subcomponent.

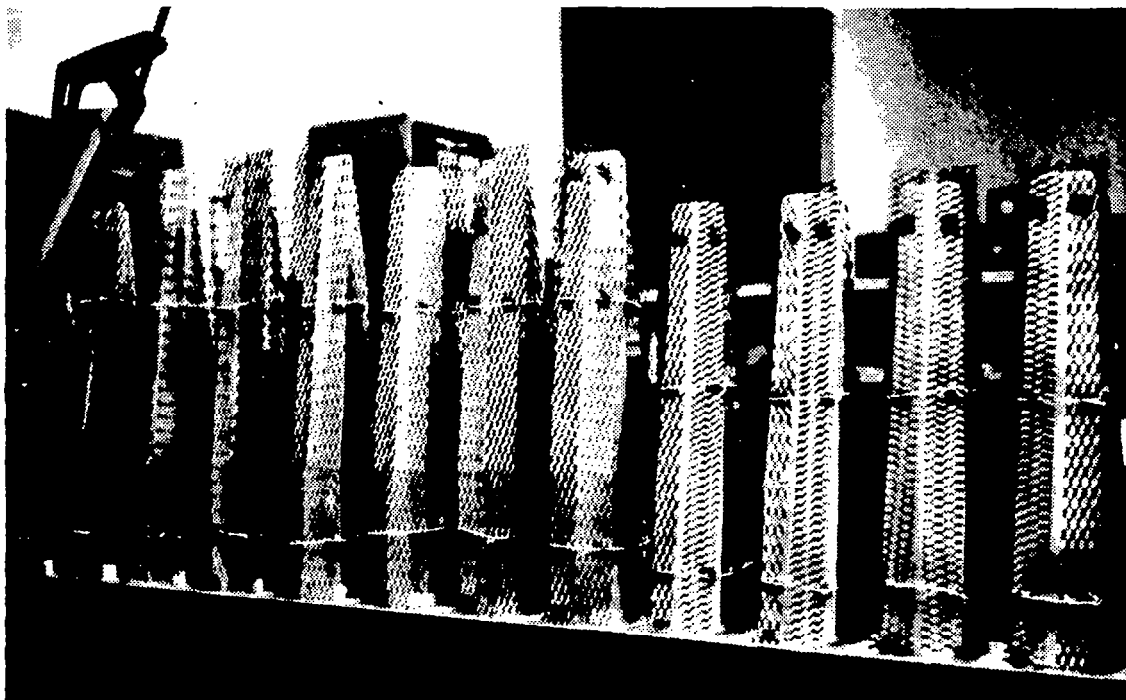


Figure 14.- Wire screen reinforcing.

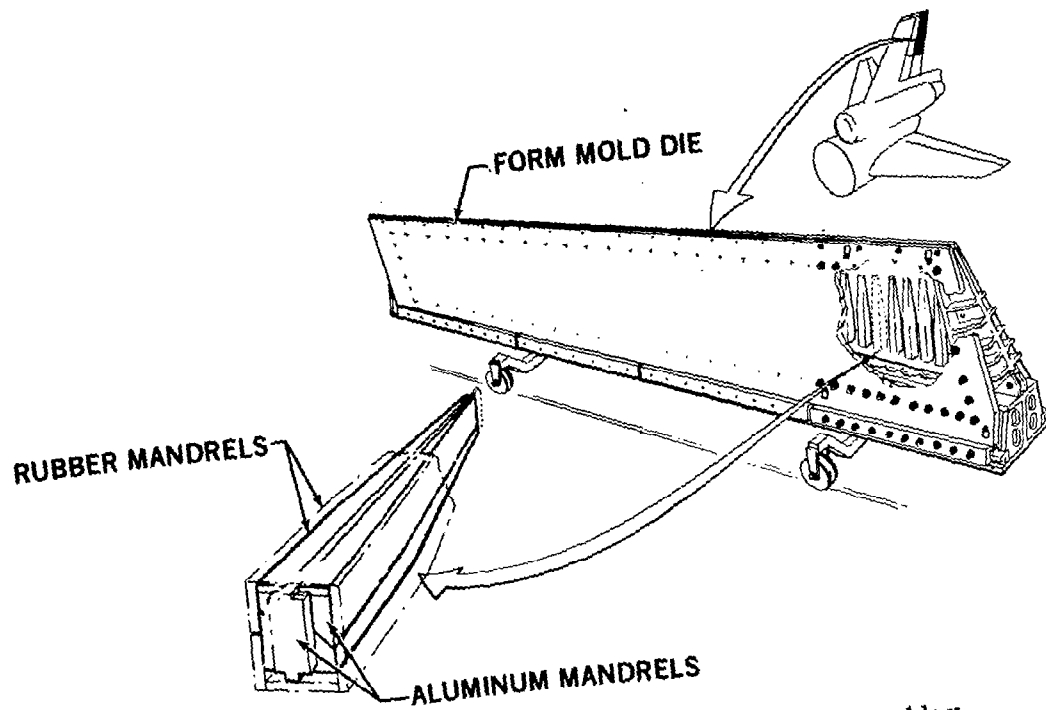
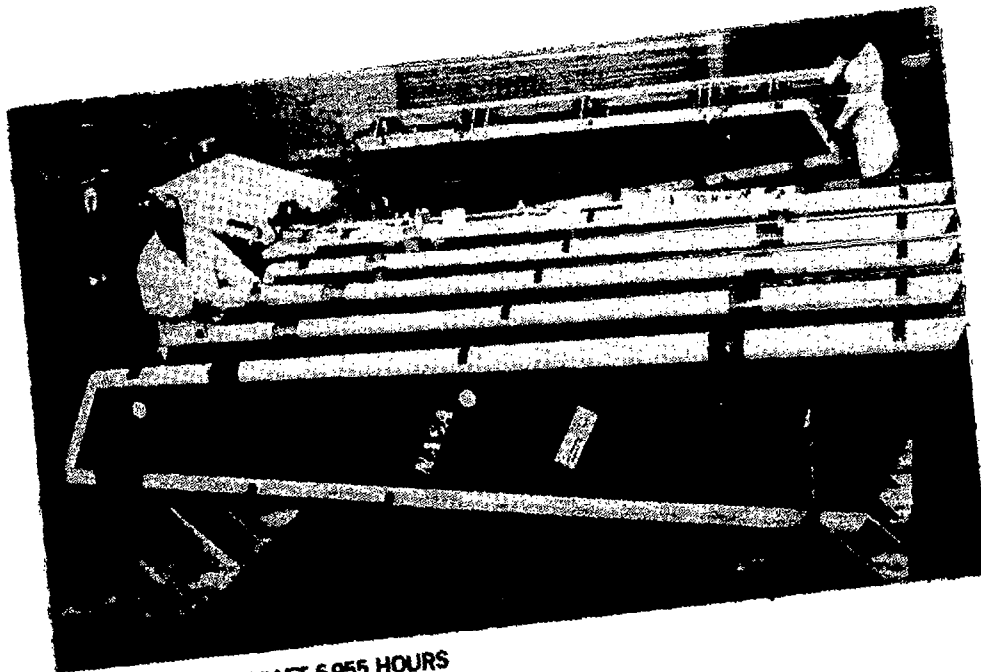


Figure 15.- Composite molding die, upper aft rudder.



- HIGH TIME AIRCRAFT 6,955 HOURS
- TOTAL FLIGHT SERVICE 30,840 HOURS
(THROUGH JANUARY 1978)

Figure 16.- Rudder flight service.

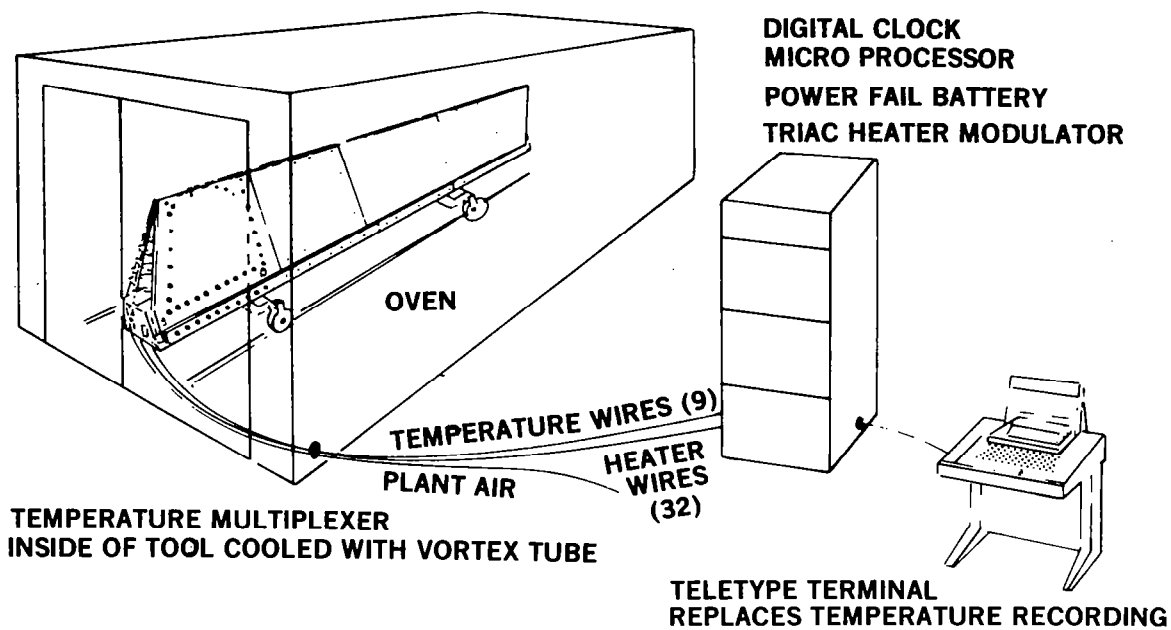


Figure 17.- Thermal temperature control system.

**TWO LOTS OF TEN EACH
DC-10 COMPOSITE RUDDER**

- 7.6-cm (3-IN.) TAPE
- BROAD GOODS TEMPERATURE CONTROL REVISED TOOLS

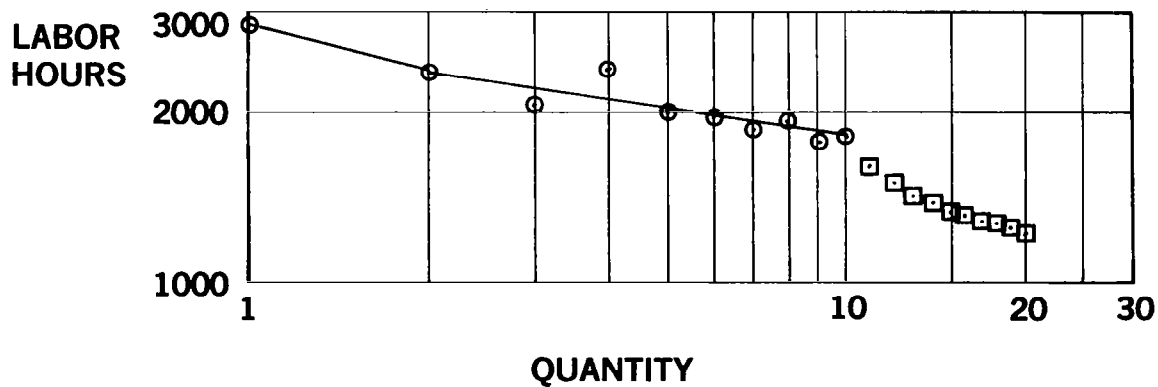


Figure 18.- Comparison of total recurring labor.

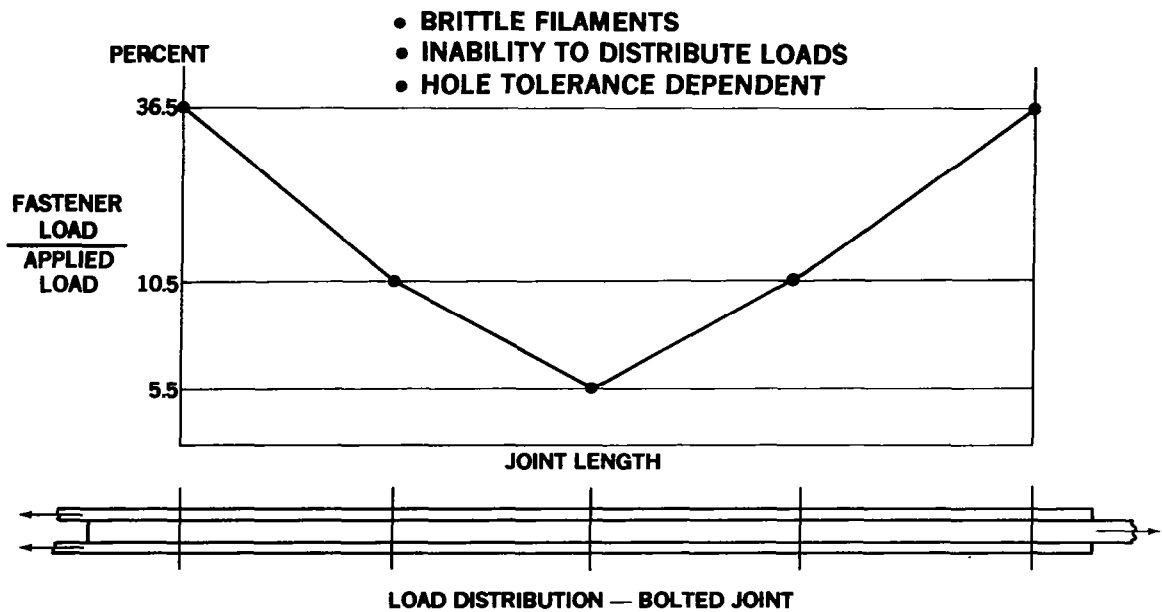


Figure 19.- Major load transfer.

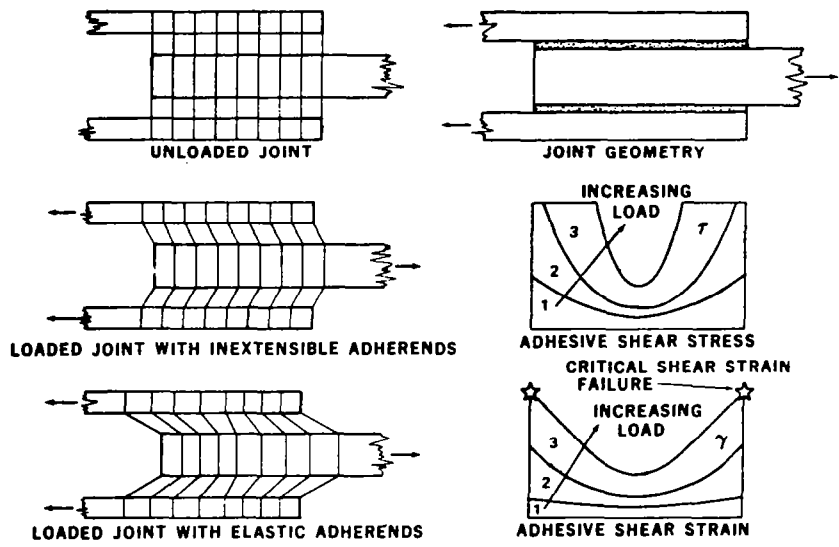


Figure 20.- Shearing of adhesive in balanced double-lap joints.

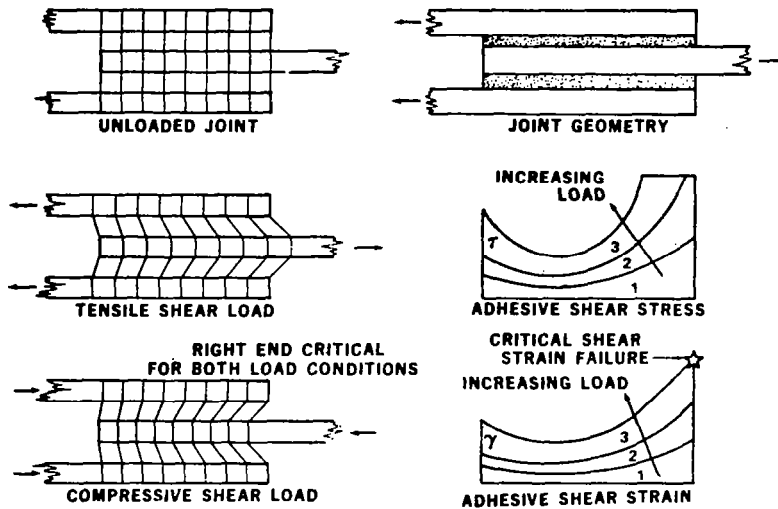


Figure 21.- Stiffness imbalance on adhesive shear.

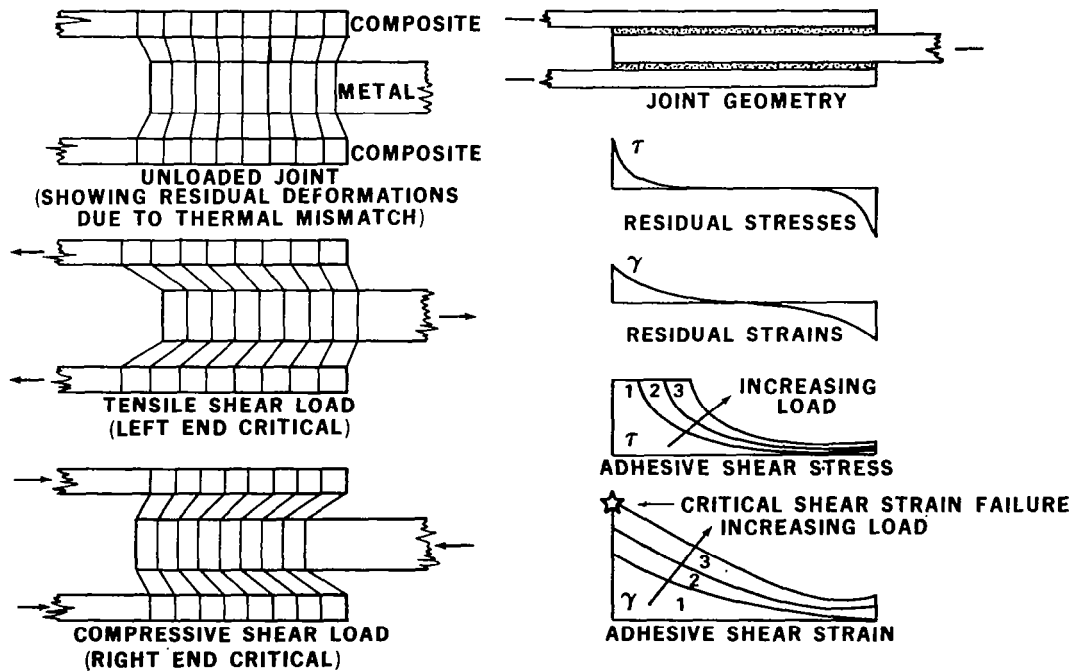


Figure 22.- Effect of adherend thermal mismatch on adhesive shear.

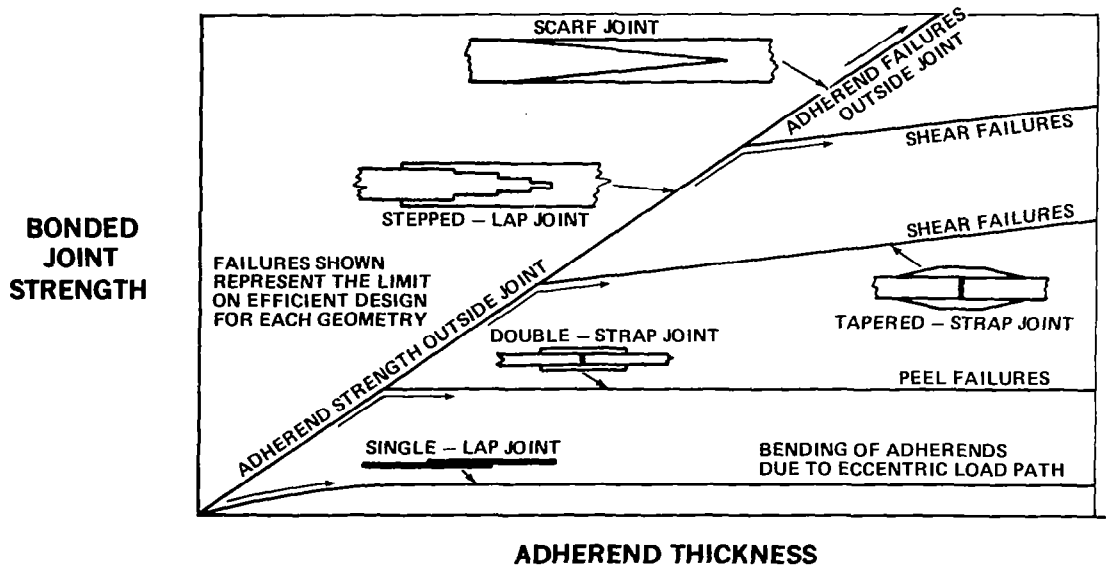


Figure 23.- Relative uses of different bonded joint types.

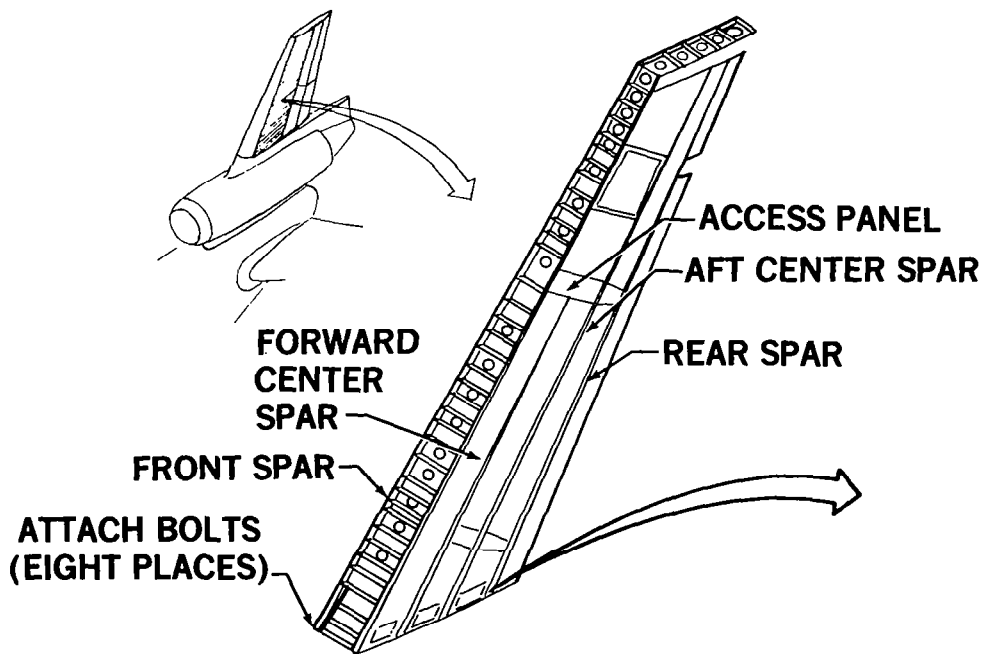


Figure 24.- DC-10 vertical stabilizer box structure.

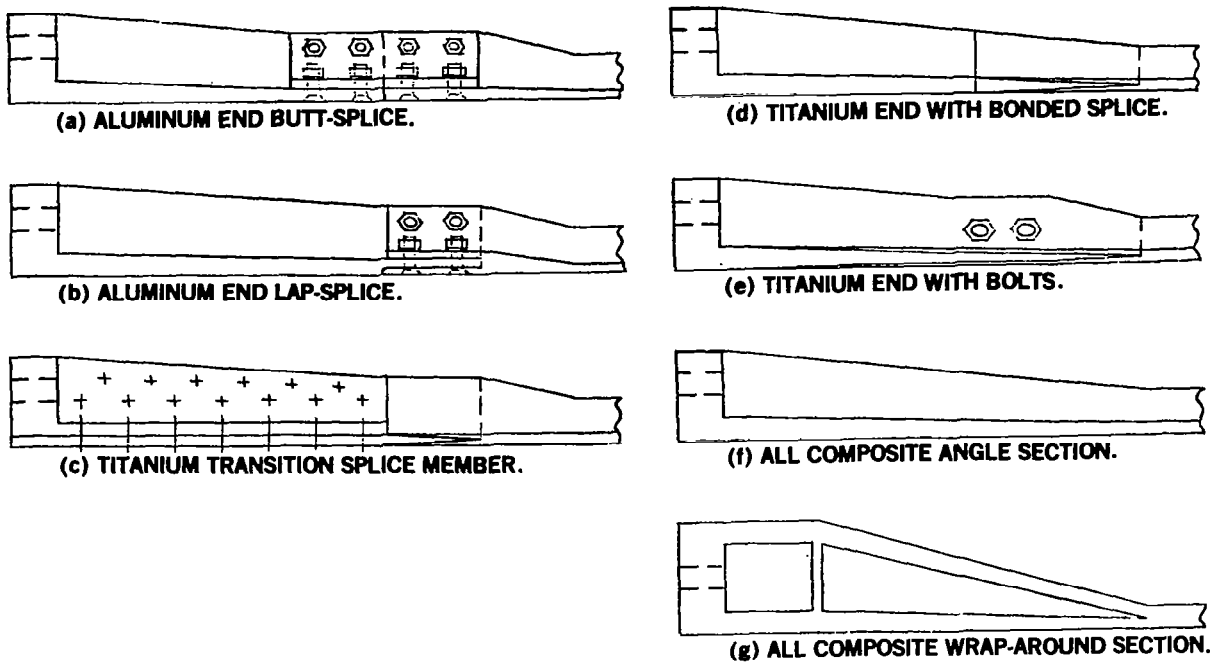


Figure 25.- Spar cap attach fitting concepts.

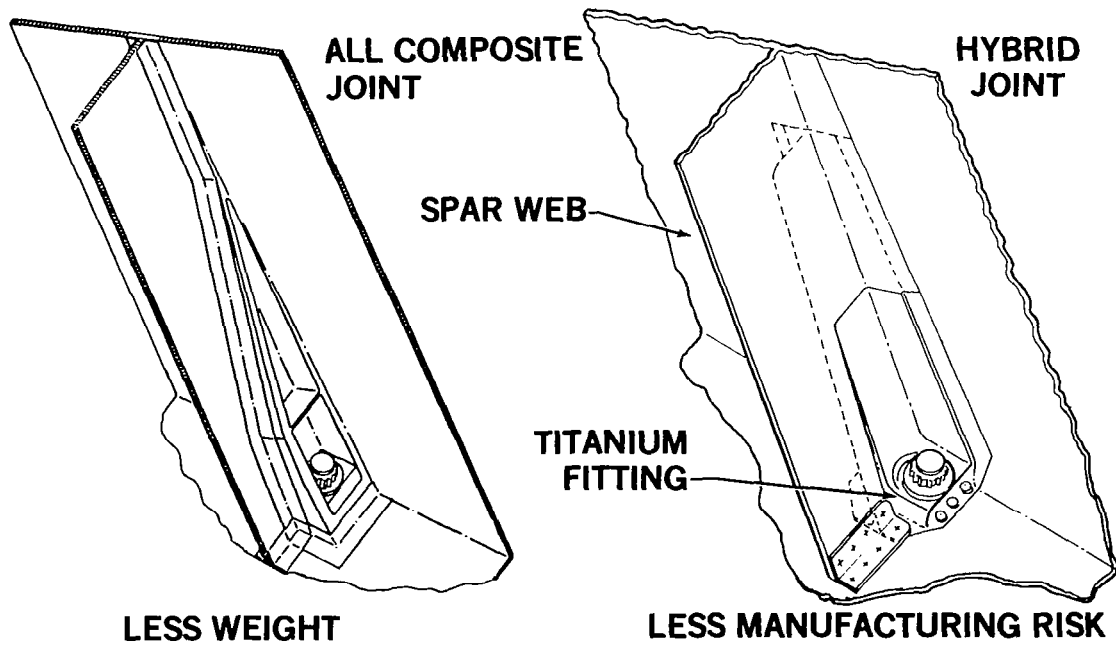


Figure 26.- DC-10 vertical stabilizer lower joint candidate design concepts.

#HALLFF
#OLD SCARF
#RUN

SCARF 09:03 JUL 01, '77

ELASTIC-PLASTIC ANALYSIS OF SCARF JOINT

INPUT DATA---ADHESIVE PROPERTIES---

G-SHEAR MODULUS
T-ADHESIVE THICKNESS
GAMMAE-ELASTIC SHEAR STRAIN
GAMMAPE-PLASTIC SHEAR STRAIN
TAUP-PLASTIC (MAX) SHEAR STRESS
?60000, .005, .1, 2.0, 6000

INPUT DATA---PROPERTIES FOR ADHEREND 1---

E1-MODULUS OF ELASTICITY
T1-THICKNESS
ALPHA1-COEFFICIENT OF THERMAL EXPANSION
?16.0E+6, .265, 4.8E-6

INPUT DATA---PROPERTIES FOR ADHEREND 2---

E2-MODULUS OF ELASTICITY
T2-THICKNESS
ALPHA2-COEFFICIENT OF THERMAL EXPANSION
?16.9E+6, .234, 0.0

INPUT DATA---OVERLAP LENGTH & TEMP DIFFERENTIAL
L-OVERLAP LENGTH
DELT-TEMPERATURE DIFFERENTIAL
?10.225, -140

ADHEREND STIFFNESS RATIO = .9327
PLASTIC TO ELASTIC STRAIN RATIO = 20.00
THERMAL MISMATCH COEFFICIENT = .555
NON-DIMENSIONALIZED OVERLAP = 24.762

TENSION CASE

AVG STRESS / MAX STRESS = 1.00000
TRANSITION POINT = 33.221
MAXIMUM LOAD (N) (4/IN) = 61350.0
SOFT END CRITICAL

COMPRESSION CASE

AVG STRESS / MAX STRESS = .99374
TRANSITION POINT = 17.836
MAXIMUM LOAD (N) (4/IN) = 60352.2
SOFT END CRITICAL

Figure 27.- Sample analysis printout for scarf joint.

